

Zero-Shot Coreset Selection via Iterative Subspace Sampling

Brent A. Griffin^{1*} Jacob Marks^{1†} Jason J. Corso^{1,2}
¹ Voxel51 ² University of Michigan

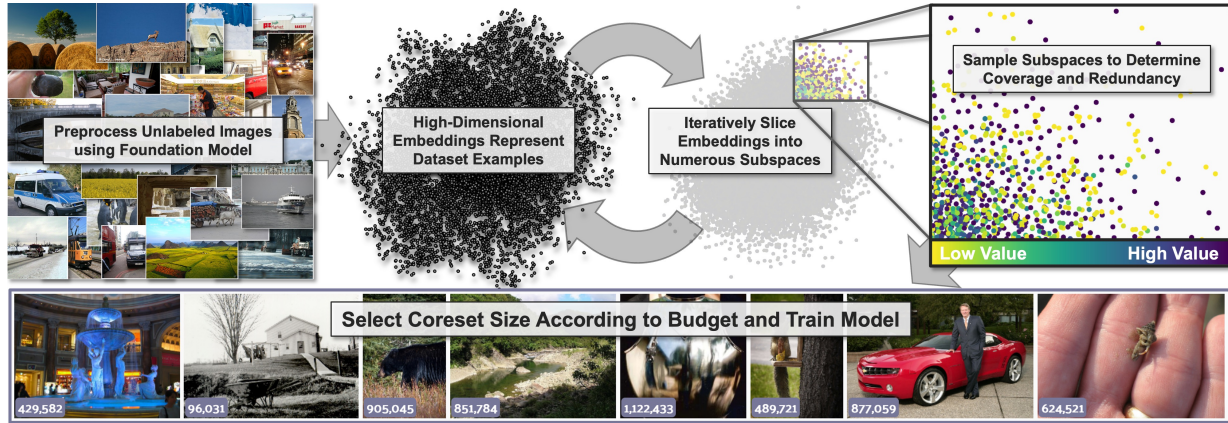


Figure 1. **Overview.** We use foundation models to generate high-dimensional embeddings for unlabeled candidate images (left). We then iteratively slice the full embedding space into subspaces (center), which we sample to find examples covering large regions of the resulting subspace distributions while penalizing redundancy (right). Finally, we output a coreset of data to train models for a given budget (bottom).

Abstract

Deep learning increasingly relies on massive data with substantial storage, annotation, and training costs. To reduce costs, coreset selection finds a representative subset of data to train models while ideally performing on par with the full data training. To maximize performance, current state-of-the-art coreset methods select data using dataset-specific ground truth labels and training. However, these methodological requirements prevent selection at scale on real-world, unlabeled data. To that end, this paper addresses the selection of coresets that achieve state-of-the-art performance but without using any labels or training on candidate data. Instead, our solution, **Zero-Shot Coreset Selection via Iterative Subspace Sampling (ZCore)**, uses previously-trained foundation models to generate zero-shot, high-dimensional embedding spaces to interpret unlabeled data. ZCore then iteratively quantifies the relative value of all candidate data based on coverage and redundancy in numerous subspace distributions. Finally, ZCore selects a coreset sized for any data budget to train downstream models. We evaluate ZCore on four datasets and outperform several state-of-the-art label-based methods, especially at low data rates that provide the most substantial cost re-

duction. On ImageNet, ZCore selections for 10% training data achieve a downstream validation accuracy of 53.99%, which outperforms prior label-based methods and removes annotation and training costs for 1.15 million images.[‡]

1. Introduction

The computational cost to train a single state-of-the-art deep learning model in various fields doubles every 3.4 months in the deep learning era due to increasingly large models and datasets [2, 56]. Since the introduction of AlexNet [23], groundbreaking models in computer vision like ViT and DALL-E all rely on massive datasets for training [13, 40]. However, there are substantial costs to collecting, storing, transmitting, and pre-processing such a vast amount of data. Furthermore, training models on vast datasets introduces yet another substantial cost for computation, sometimes hundreds of thousands of GPU hours to achieve satisfactory performance, which frustrates applications requiring repeat training over datasets such as hyperparameter optimization [25, 28] and neural architecture search [14, 24].

Increasing data efficiency mitigates these deep learning challenges. Specifically, coreset selection reduces the

* Corresponding email: brent@voxel51.com.

† Work completed while Jacob Marks was at Voxel51.

‡ Code available at <https://github.com/voxel51/zcore>.

training set size by selecting a pruned subset that contains only valuable examples (the *core set*), such that downstream models trained on the coresets achieve similar performance to those trained on the original, full dataset [15].

Coreset selection methods have demonstrated impressive results using median class values [50], diverse coverage of importance scores [58], and gradient dynamics during training [54]. Notably, to achieve maximum performance in experiments, these and other state-of-the-art coreset methods increasingly use data labels and training prior to selection [16, 18]. However, the majority of real-world data are unlabeled. Moreover, labeling all candidate images to consider them for selection is cost prohibitive, with annotation taking anywhere between 7 seconds per bounding box to 1.5 hours for full semantic segmentation [11, 20].

Unlabeled coreset selection uniquely reduces label costs by pruning away data prior to *any* labeling. If the downstream model is self-supervised, no labels are required. If the downstream model is supervised, *only* the coreset is labeled. Notably, some coreset methods use self-supervised learning in place of label-based training [44, 59], but this still requires substantial time and compute to make selections at scale. Furthermore, coupling selection with training on a single model architecture decreases generalization.

To that end, this paper addresses the problem of selecting coresets that achieve state-of-the-art performance *without* using labels or training, enabling low-cost data selection at scale. Our approach, **Zero-Shot Coreset Selection** via Iterative Subspace Sampling (**ZCore**), uses previously-trained foundation models to process images in a single forward pass, generating a high-dimensional embedding space representation of all unlabeled data. **ZCore** then iteratively slices the full embedding space down to numerous low-dimensional subspaces that are sampled via Triangular distribution to estimate each data example’s value based on *coverage* and *redundancy* (see Fig. 1). Each subspace contains a unique combination of foundation model features and reduces runtime relative to full embedding space processing. Notably, our default **ZCore** implementation uses 818,560 diverse subspaces and completes coreset selections for all possible prune rates on CIFAR100 in 381.6s using a standard laptop. Our contributions are:

1. Formalizing and contrasting labeled and unlabeled coreset selection, with the later substantially reducing data- and label-based costs for efficient deep learning at scale.
2. Developing the **ZCore** method, which selects coresets from unlabeled data with efficient computation at scale using a novel iterative subspace sampling technique.
3. Evaluating **ZCore** with the state-of-the-art using ten prior coreset methods and four datasets. Results show that **ZCore** performs best in multiple low-data rate cases and overall outperforms all label-based methods save one, without **ZCore** using labels or training for selection.

4. Evaluating **ZCore** under constant algorithmic settings across a dataset and coreset selection scale greater than three orders of magnitude. To our knowledge, there is no precedent for this selection range of experiments and generalization in the coreset selection literature.

From these results, **ZCore** establishes a new state-of-the-art.

2. Related Work

Dataset Distillation is similar to coreset selection in that it supports data-efficient deep learning. On a functional level, the objectives of many coreset methods also apply to dataset distillation. However, as opposed to selecting a subset of *existing* data for a coreset, dataset distillation aims to generate a much smaller dataset with *synthetic* examples that yield the same performance as the larger initial dataset [53]. Notable dataset distillation methods generate synthetic examples relative to the initial dataset by matching gradients [57], differentiable Siamese augmentation for better synthesis [55], aligning features [47], multi-step parameter matching [7], and embedding space distribution matching [56]. These dataset distillation methods are remarkable for creating small but effective synthetic training datasets. Alternatively, to utilize real-world data, our current work selects and evaluates coresets from already existing data.

Active Learning is another research area that supports data-efficient deep learning by enabling learning algorithms to choose their own data to improve performance with less training [42], which is especially useful when large portions of data are unlabeled and labeling data is expensive [5]. In fact, active learning encompasses the particularly hard problem of starting selection without initial labeled examples, i.e., the cold start problem [29]. Notably, some recent active learning methods focus on the importance of coverage diversity in data selection [3, 9]. However, these methods iteratively train and select data on an increasing set for a specific model. Alternatively, our work selects data without initial labels for a *single, model-agnostic* training phase.

Coreset Selection prunes datasets down to a smaller, valuable *core set* to reduce costs and enable data-efficient deep learning. A basic solution to find the optimal coreset is to search through and train on every subset to find the best corresponding model performance. However, this simple approach is NP-hard, leading to the development of many alternative coreset methods. Early coreset methods aim for a consistent data distribution to the full dataset [4, 15], e.g., greedily adding one sample at a time to match embedding space centers [49]. Other coreset methods can be broadly categorized as selecting by optimization [48, 52], coverage or diversity [41, 51, 58], semantic redundancy [1, 43], and importance criteria [45, 46]. Recent coreset innovations address ongoing challenges like application on a wide range of dataset sizes [50], making selections on data with label errors [34], and best use of full training dynamics [54, 59].

Table 1. Comparison of **Data and Procedural Requirements**.

State-of-the-art Coreset Methods	Selects Coreset <i>Without</i> :		
	Training Data	Ground Truth Labels	Prune on Truth Specific Tuning
ZCore (ours)	Yes	Yes	Yes
Protypesss [44] <small>NeurIPS 2022</small>	No	Yes	Yes
ELFS [59] <small>ICLR 2025</small>	No	Yes	No
Dyn-Unc [18] <small>CVPR WS '24</small> , Moderate [50] <small>ICLR 2023</small>	No	No	Yes
TDDS [54] <small>CVPR 2024</small> , Coverage [58] <small>ICLR 2023</small>	No	No	No

Our current work is inspired by the success of previous coreset selection methods. Importantly, recent state-of-the-art methods have increasingly improved coreset performance (especially at low data rates) through the use of labels and/or training on the larger initial dataset (see Tab. 1, Fig. 2). Instead, our current work maintains or improves state-of-the-art coreset selection performance using only unlabeled data and no dataset- or architecture-specific training. Fundamentally, this coreset approach broadens applicability to new data and models while reducing label error sensitivity, labeling costs, and computation at scale.

3. Problem Formulation

We first define the problem of *labeled* coreset selection. Formally, we are given a labeled dataset $\mathbb{S}^l = \{(\mathbf{x}_i, y_i)\}_{i=1}^N$ with N examples drawn i.i.d. from an underlying distribution P , where \mathbf{x}_i are the data and y_i is the ground truth label for each example. The goal is to select a subset of \mathbb{S}^l to reduce future storage and training consumption while closely maintaining the performance of full dataset training. We denote this *coreset* as $\mathbb{S}^c = \{(\mathbf{x}_i, y_i)\}_{i=1}^n \subset \mathbb{S}^l$, which has n examples and a *prune rate* of $1 - \frac{n}{N}$. We formulate coreset selection as [41]:

$$\arg \min_{\mathbb{S}^c \subset \mathbb{S}^l | 1 - \frac{n}{N} \geq p} \mathbb{E}_{\mathbf{x}, y \sim P} [l(\mathbf{x}, y; f(\mathbb{S}^c))], \quad (1)$$

where p is a prune rate set *before* training, l is the loss function, and $f(\mathbb{S}^c)$ is a model trained on \mathbb{S}^c . Notably, many SOTA methods select \mathbb{S}^c by assigning an importance score to each example [54, 59], which we denote as $\mathbf{s} \in \mathbb{R}^N$.

We now define the problem of *unlabeled* coreset selection for data- and *label*-efficient deep learning. Formally, given an unlabeled dataset $\mathbb{S} = \{\mathbf{x}_i\}_{i=1}^N$, the goal is to select $\mathbb{S}^c \subset \mathbb{S}$ without using *any* ground-truth label y_i . The motivation for this change is that it is preventative to label an entire massive dataset when much of the data will be pruned. We formulate unlabeled coreset selection by replacing $\mathbb{S}^c \subset \mathbb{S}^l$ with $\mathbb{S}^c \subset \mathbb{S}$ in Eq. (1). Notably, after selecting \mathbb{S}^c , *if* the downstream model $f(\mathbb{S}^c)$ is supervised, we use only n labels for the coreset as $\mathbb{S}^c = \{(\mathbf{x}_i, y_i)\}_{i=1}^n$.

Along with the aforementioned benefits of coreset selection, unlabeled coreset selection uniquely increases scale and reduces labeling costs. First, while we can use any \mathbf{x}_i

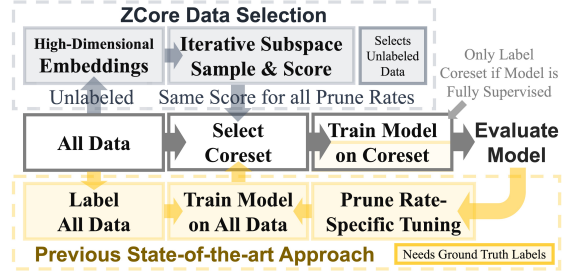


Figure 2. Coreset and Model Train Workflow Comparison.

from a labeled dataset \mathbb{S}^l , we can also extensively sample and consider more examples \mathbf{x} from the underlying distribution P without any annotation or labeling requirements. This extension enables us to source coresets from a much larger initial dataset. In effect, unlabeled coreset selection extends selection to the majority of unlabeled, real-world data. Second, for supervised model training, we only label the n coreset examples after they are selected, so there is a $N - n$ reduction in labeling costs relative to label-based selection. On ImageNet, unlabeled selection at a 90% prune rate removes label requirements for 1.15 million images.

Finally, we likewise note that selecting examples without training on candidate data substantially improves runtime.

4. Zero-Shot Coreset Selection via Iterative Subspace Sampling

We use the unlabeled coreset selection formulation to develop a new method of **Zero-Shot Coreset Selection** via Iterative Subspace Sampling (ZCore). In place of label- or training-based selection, ZCore first uses foundation models to generate a zero-shot, high-dimensional embedding space representation of the full dataset (Sec. 4.1). ZCore then samples varying, lower-dimensional embedding subspaces to efficiently determine which examples provide valuable coverage across unique feature combinations (Sec. 4.2). Subsequently, ZCore determines which examples in proximity to those providing coverage are redundant (Sec. 4.3). Finally, ZCore uses the coverage and redundancy metrics to iteratively sample and score each candidate training example to determine final coreset selections (Sec. 4.4).

4.1. Foundational Embedding Representation

ZCore selects data using a zero-shot, high-dimensional embedding space representation of unlabeled dataset \mathbb{S} . We generate embeddings using a foundation model denoted as $f(\cdot) = g(h(\cdot))$, where h is the model component mapping input data to hidden representations at the penultimate layer and g maps the embedding space to a previously learned output f . We use $h(\mathbf{x}_i) \in \mathbb{R}^M$ to generate an M -dimension *embedding space* for input data $\mathbb{S} = \{\mathbf{x}_i\}_{i=1}^N$ denoted as

$$\mathbf{Z} = [h(\mathbf{x}_1), \dots, h(\mathbf{x}_N)] \in \mathbb{R}^{N \times M}. \quad (2)$$

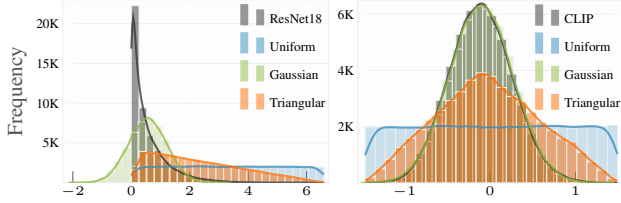


Figure 3. **Comparison of embeddings and sampling techniques.** ResNet18 (left) and CLIP (right) are the first-dimension model embeddings for 50,000 CIFAR100 train set examples, while each corresponding distribution type is sampled 50,000 times.

Embedding space \mathbf{Z} lets us use the previously learned hidden representation of h as a zero-shot alternative to label- or training-based coreset selection. In general, examples corresponding to different classes or concepts map to different regions of the feature-based embedding space. Thus, we quantify the importance of each example in terms of relative coverage and redundancy in \mathbf{Z} as a representation of the underlying data distribution $\mathbf{x}, y \sim P$ in Eq. (1). **Remarks on \mathbf{Z} :** In Sec. 5 experiments, we generate all model embeddings in advance using off-the-shelf weights for a ResNet18 [17] and CLIP ViT-L-14 model [39], which we concatenate as $h(\mathbf{x}_i) = \begin{bmatrix} h^{\text{RN18}}(\mathbf{x}_i) \\ h^{\text{CLIP}}(\mathbf{x}_i) \end{bmatrix} \in \mathbb{R}^{1,280}$. As we will show in Sec. 5.3, relative to coreset methods using full dataset training for 60-200 epochs, generating embeddings takes much less time as it only requires one forward pass per sample, a subcomponent (h) of the full model architecture, and no training-based back propagation or metric tracking.

4.2. Coverage of Embedding Subspaces

Our first objective for coreset selection is to select examples that maximize coverage of embedding space \mathbf{Z} . To quantify coverage, we develop a Monte Carlo-inspired sampling technique [31], which estimates the relative contribution of each candidate training example $\mathbf{x}_i \in \mathbb{S}$ in covering a carefully-designed distribution over the embedding space.

We assume a Triangular distribution over each embedding space dimension $j \in \{1, \dots, M\}$ using

$$z_j \sim p(x, j) := \begin{cases} \frac{2(x - z_j^{\min})}{(z_j^{\max} - z_j^{\min})(z_j^{\text{med}} - z_j^{\min})} & \text{for } z_j^{\min} \leq x < z_j^{\text{med}} \\ \frac{2(z_j^{\text{med}} - x)}{(z_j^{\max} - z_j^{\min})(z_j^{\max} - z_j^{\text{med}})} & \text{for } z_j^{\text{med}} \leq x \leq z_j^{\max} \end{cases}, \quad (3)$$

$$\mathbf{z} := [z_1, \dots, z_M]^T \in \mathbb{R}^M,$$

where \mathbf{z} is a full random sample from the distribution of \mathbf{Z} across all M dimensions, $\mathbf{z}^{\min} = \{\min(\mathbf{Z}_{:,j})\}_{j=1}^M \in \mathbb{R}^M$ is the minimum \mathbf{Z} value for each embedding dimension, and $\mathbf{z}^{\text{med}}, \mathbf{z}^{\max} \in \mathbb{R}^M$ are the corresponding median and maximum \mathbf{Z} values. In practice, Triangular distribution Eq. (3) robustly covers both exponential- (ResNet) and Gaussian-

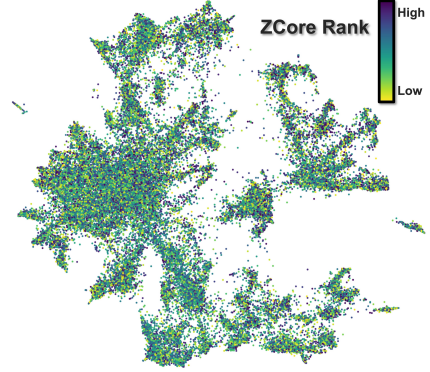


Figure 4. **ZCore Coreset Rank Visualization** for CIFAR100. Model embeddings and 2D approximation of the full embedding space generated using the FiftyOne Library and UMAP [30, 32].

shaped (CLIP) embedding distributions (see Fig. 3). Relative to uniform or Gaussian, the Triangular distribution uniquely achieves all objectives of: providing sufficient coverage for densely populated regions of the embedding space, covering outliers, and not sampling empty space.

We increase sample efficiency over $\mathbf{Z} \in \mathbb{R}^{N \times M}$ by reducing its dimensionality to $\mathbb{R}^{N \times m}$ subspaces using

$$\begin{aligned} \mathbf{D} &:= [\mathbf{1}_{d_1}, \dots, \mathbf{1}_{d_m}] \in \mathbb{N}^{M \times m}, \\ \hat{\mathbf{Z}} &:= \mathbf{Z}\mathbf{D} \in \mathbb{R}^{N \times m}, \end{aligned} \quad (4)$$

where \mathbf{D} linearly maps \mathbf{Z} to m reduced embedding dimensions ($m \leq M$), $\{d_1, \dots, d_m\} \in \mathbb{N}$ is a set of m random indices chosen without replacement from $\{1, \dots, M\}$, and $\mathbf{1}_i$ is a one-hot vector with i -th element equal to 1. We use Eq. (4) to generate numerous subspaces $\hat{\mathbf{Z}}$ that are computationally efficient, diverse, and cover \mathbf{Z} in the aggregate. We also use Eq. (4) in Eq. (3) to reduce the dimension of random sampling from $\mathbf{z} \in \mathbb{R}^M$ to $\hat{\mathbf{z}} := \mathbf{z}\mathbf{D} \in \mathbb{R}^m$.

We quantify coverage for each random subspace sample $\hat{\mathbf{z}}$ by finding the closest *existing* dataset example

$$\arg \min_i \|\hat{\mathbf{z}} - \hat{\mathbf{Z}}_i\|_1, \quad (5)$$

where we denote k as the solution to i in Eq. (5) and $\hat{\mathbf{Z}}_k$ is the dataset example closest to $\hat{\mathbf{z}}$. Finally, we quantify an importance score specifically for coverage (s^c) as

$$s_i^c := \begin{cases} 1 & \text{for } i = k \\ 0 & \text{otherwise} \end{cases}, \quad (6)$$

$$\mathbf{s}^c := [s_1^c, \dots, s_N^c] \in \mathbb{R}^N,$$

where s^c adds to the estimated embedding coverage value for dataset example k . We repeat our process of randomly selecting \mathbf{D} , sampling $\hat{\mathbf{z}}$, and adding coverage for the closest examples across many iterations to extend the coverage score across all examples in \mathbb{S} . Unlike random sampling,

our coverage score rewards hard examples that individually occupy large, unique, low-density areas of the embedding space (see Fig. 4), which improves coreset performance.

Remarks on m : In Sec. 5 experiments, we choose $m = 2$ (s.t. $D \in \mathbb{R}^{M \times 2}$) random embedding dimensions per sample \hat{z} , which decreases runtime, generates $\binom{M}{2} \approx \frac{M^2}{2}$ unique 2D subspaces from Z , and optimizes ZCore selection performance (see Tab. 3 and Fig. 13 in Supplementary).

4.3. Removing Embedding Subspace Redundancy

To avoid redundant coreset selection in embedding subspaces, we develop a redundancy metric that operates subsequently to each coverage solution k in Eq. (5). Specifically, for each coverage example \hat{Z}_k , we quantify a redundancy penalty for the set of $\mathbb{K} \in \mathbb{N}^\alpha$ nearest neighbors as

$$v_i^R := \begin{cases} (\|\hat{Z}_k - \hat{Z}_i\|_1)^{-\beta} & \text{for } i \in \mathbb{K} \\ 0 & \text{otherwise} \end{cases}, \quad (7)$$

$$\mathbf{s}^R := [s_1^R, \dots, s_N^R] = \frac{\mathbf{v}^R}{\|\mathbf{v}^R\|_1} = \frac{[v_1^R, \dots, v_N^R]}{\|\mathbf{v}^R\|_1} \in \mathbb{R}^N,$$

where exponent β determines the rate of penalty changes between \hat{Z}_k 's α nearest neighbors with varying distance $\|\hat{Z}_k - \hat{Z}_i\|_1$ and $\|\mathbf{v}^R\|_1 \in \mathbb{R}$ normalizes our redundancy score \mathbf{s}^R so that the coverage and redundancy scores for each sample iteration are balanced as $\|\mathbf{s}^R\|_1 = \|\mathbf{s}^C\|_1 = 1$.

Remarks on α, β : In Sec. 5 experiments, we choose $\alpha = 1,000$ to decrease runtime of Eq. (7) on large datasets while still reaching many examples per iteration, and we choose $\beta = 4$ to ensure that primarily the closest neighbors to each \hat{Z}_k are substantially estimated as redundant.

4.4. Iterative Sampling for Coreset Selection

Using the embedding subspace sampling process (D and \hat{Z} in Eq. (4), \hat{z} and k in Eq. (5)) and subsequent coverage and redundancy metrics (\mathbf{s}^C in Eq. (6), \mathbf{s}^R in Eq. (7)), we define our final coreset importance score $\mathbf{s} \in \mathbb{R}^N$ as

$$\mathbf{s} := \mathbf{s} + \sum_{t=1}^T \mathbf{s}_t^C(k_t) - \mathbf{s}_t^R(k_t), \quad (8)$$

where $\mathbf{s} = \{s_i \sim \mathcal{U}[0, 1]\}_{i=1}^N$ is a random initialization for each example, k_t is the example solution in Eq. (5) at iteration t for subspace \hat{Z}_t and sample \hat{z}_t , $\mathbf{s}_t^C(k_t)$ and $\mathbf{s}_t^R(k_t)$ are the corresponding coverage and redundancy scores for k_t , and T is the total number of sample and score iterations. Notably, \mathbf{s} promotes inclusion of a few examples outside of our primary coverage and redundancy metrics and each iteration t is independent, enabling us parallelize and accelerate ZCore score computation.

Finally, after computing score \mathbf{s} to estimate the relative value of each example in unlabeled dataset \mathbb{S} , we select the n examples with highest scores (corresponding to ‘‘High’’

rank in Fig. 4) as our final coreset for downstream model training. Notably, we use the same \mathbf{s} for all prune rates.

For experiments in Sec. 5, we also use \mathbf{s} to weight the loss and gradient for downstream model training using

$$\mathbf{w} = \frac{\mathbf{s} - \min(\mathbf{s})}{\max(\mathbf{s}) - \min(\mathbf{s})}, \quad (9)$$

where $\mathbf{w} = [w_1, \dots, w_N]^\top \in \mathbb{R}^N$, $w_i \in [0, 1]$, and the loss is scaled each batch by the mean w_i score corresponding to the specific training examples in that batch. Essentially, we already determine how valuable each example is for coreset selection and want to influence model training accordingly.

5. Evaluation

5.1. Experimental Setup

Datasets. We evaluate ZCore selections for downstream model training and subsequent validation accuracy on four image classification datasets: CIFAR10 [22], CIFAR100, ImageNet [12], and EuroSAT [19]. Notably, full dataset sizes span from 1.3 M to 2,700 examples and coreset sizes span from 896,817 to 270 examples (over three orders of magnitude, see Tab. 4 in Supplementary). EuroSAT has no explicit training set, so we create ‘‘four’’ datasets using 80/20, 40/60, 20/80, and 10/90 training/validation splits to experiment with decreasing dataset scale in the same distribution of satellite images. All reported accuracy results are for model validation after training on a specific coreset.

Network Training. We use two different network models and training regimes to evaluate coresets. For CIFAR10, CIFAR100, and EuroSAT, we train a ResNet18 model on selected coresets for 200 epochs with a batch size of 128. For ImageNet, we alternatively train a ResNet32 model for 60 epochs with a batch size of 256. Following the protocol of [54], we use an SGD optimizer with momentum 0.9, weight decay 0.0005, and a learning rate of 0.1 that decays with the cosine annealing scheduler via PyTorch [36]. After model training, we use the model’s validation accuracy to quantitatively evaluate coreset selection performance.

ZCore & Baselines. We implement ZCore using the Sec. 4 formulation with constant parameter settings across all datasets and prune rates. We compare ZCore against the state-of-the-art using ten previous coreset selection methods: **Entropy** [10], **Forgetting** [46], **EL2N** [37], **AUM** [38], **Moderate** [50], **Dyn-Unc** [18], **TDDS** [54], **Prototypes_{sup.}** [44], **Prototypes_{ss.}** [44], and **ELFS** [59]. ZCore is the only method to make selections without labels or data training (see Fig. 2) aside from **Random**, which selects examples with uniform random sampling. In place of label-based training, Prototypes_{ss.} and ELFS make selections after self-supervised training on candidate data. Detailed method descriptions and runtime & label efficiency comparisons are provided in the Supplementary Material.

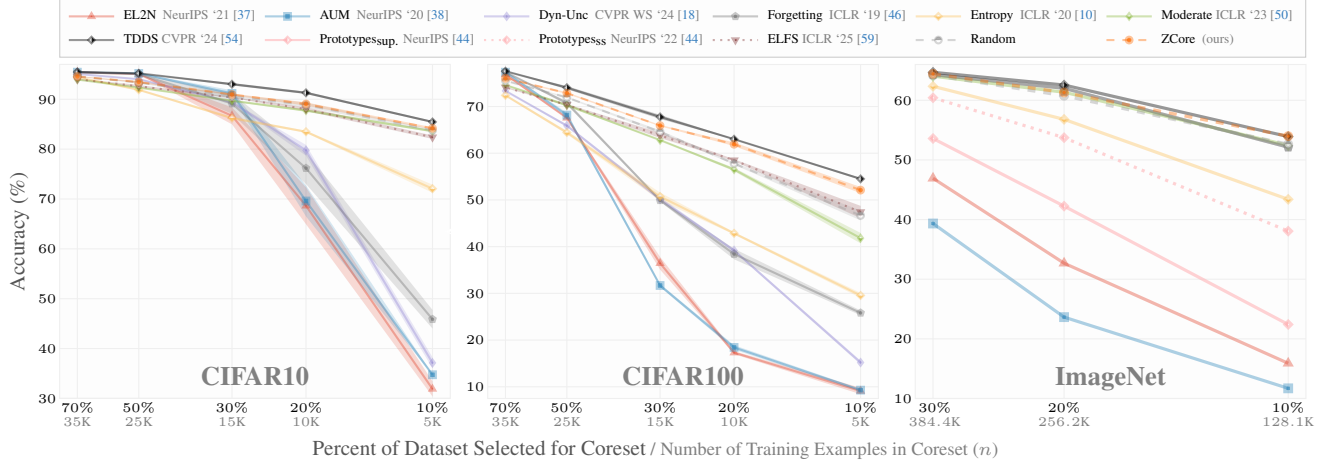


Figure 5. Comparison of coreset selection methods using downstream model validation on **CIFAR10**, **CIFAR100**, and **ImageNet**. Method results with solid lines select coreset data using labels and training, method results with dotted lines select coreset data using self-supervised training, and method results with dashed lines select coreset data without labels *or* training. The x -axis is in log scale for the number of coreset examples used for model training. Corresponding result tables for each dataset are provided in the Supplementary Material.

5.2. Quantitative Coreset Performance Comparison

CIFAR Datasets. We provide coreset selection results for CIFAR10 (10 classes) and CIFAR100 (100 classes) in Fig. 5 (50,000 images each). Full dataset training on the ResNet18 model achieves 95.23% (CIFAR10) and 78.21% (CIFAR100) accuracy. Despite making selections without labels or training, ZCore achieves the second best overall performance, staying relatively competitive with SOTA label- and training-based TDDS selections all the way through the lowest 10% data rate. Meanwhile, most coreset methods exhibit a substantial performance drop at 30% data selection on CIFAR100 and at 20% selection on CIFAR10.

ImageNet Dataset. We provide coreset selection results for ImageNet (1,000 classes) in Fig. 5. Full dataset training (1.28M images) on the ResNet32 model achieves 73.54% accuracy. ZCore and TDDS coreset selections achieve the best overall performance, establishing consistent performance on a larger, more difficult dataset. Notably, ZCore selects the best performing coreset at the 10% data selection rate, reducing costs for 1.15M pruned images.

Decreasing Dataset Size on EuroSAT. We provide coreset selection results for all EuroSAT dataset splits in Fig. 6, which evaluates coreset selection at a decreasing scale on satellite images (all 10 classes). Full dataset training on the ResNet18 model achieves 98.59% (EuroSAT80, 21,600 images), 98.20% (EuroSAT40, 10,800 images), 97.36% (EuroSAT20, 5,400 images), and 93.64% accuracy (EuroSAT10, 2,700 images). Overall, ZCore cuts much of the performance gap between Random and TDDS selections. For the 10% selection rates, ZCore outperforms TDDS on EuroSAT40 but has a lower accuracy than TDDS and Random on EuroSAT20 and EuroSAT10, where the pruned coresets only have 540 and 270 training examples. No-

Table 2. **Comparison of Coreset Selection Efficiency** on CIFAR100 for 70%, 30%, and 10% data rates. Selection “Total” is the runtime to generate all three coresets. Runtimes use a standard M3 Max-equipped “Laptop” or a single L40S “GPU” on a Lambda Scalar. ELFS hardware requirements prohibit laptop experiments. Model training and full details provided in Supplementary Tab. 5.

Setup	Selection Runtime (s)				Train Labels				
	Components			Total	70%	30%	10%		
ZCore	Embedding		Generation		ZCore Score				
	ResNet18	CLIP	Parallel	Score					
	Laptop	635	6,471	6,471		382	35K	15K	5K
GPU	145	97.0	145	54.7	6,853	35K	15K	5K	
TDDS	Train		TDDS Score						
	Dynamics	70%	30%	10%					
	Laptop	188,295	27.0	25.5	0.9	188,296	50K	50K	50K
	GPU	1,540	22.6	20.9	1.3	1,541	50K	50K	50K
ELFS	DINO		Pseudo		ELFS				
	Embed	Deep	Cluster	Train	Score				
	Laptop	—	—	—	—	—	—	—	
	GPU	111	1,093	1,476	30.3	7,908	35K	15K	5K

tably, unlike TDDS, ZCore uses constant parameter settings across all prune rates. On the other hand, ZCore small dataset performance improves with alternative settings (e.g., reducing number of neighbors for redundancy in Eq. (7)).

5.3. Quantitative Coreset Efficiency Comparison

We compare runtime and label efficiency of TDDS (labeled training-based selection), ELFS (label-free training-based selection), and ZCore (no labels *or* training) in Tab. 2.

For runtime, ZCore selects the three CIFAR100 coresets $27.5\times$ faster than TDDS on a laptop and $39.6\times$ faster than ELFS on a GPU. In reality, the relative time to implement ZCore is even faster. Reason being, ZCore does not use hyperparameter searches to determine unique settings for each dataset and prune rate. Instead, ZCore uses the exact same settings across all datasets and the exact same score across

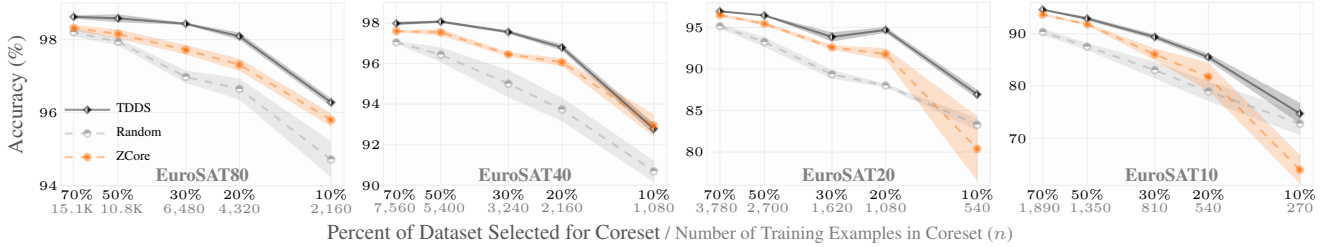


Figure 6. Comparison of coreset methods using downstream model validation on 80/20, 40/60, 20/80, and 10/90 training/validation splits of EuroSAT. Only TDDS selects data using labels and training. Corresponding results Tab. 10 is provided in the Supplementary Material.



Figure 7. Top-10 ZCore Selection Scores (orange) for EuroSAT80 (top), CIFAR100 (middle), and ImageNet (bottom).

all prune rates. On the other hand, both comparison methods perform parameter searches on *each* dataset *and* prune rate to determine their final dataset- and prune-specific settings. It is cost-prohibitive to replicate the hyperparameter search of each comparison method for our experiments in Tab. 2, but as one example, ELFS’s developers report it takes approximately 17 hours using four A6000 GPUs to find a single prune rate setting on ImageNet [59].

For label efficiency, TDDS uses ground truth labels on all candidate data prior to selection. On the other hand, ZCore and ELFS only use labels for downstream model training on the selected coreset. Thus, TDDS requires 1.4, 3.3, and $10\times$ more labels than ZCore to train models at the respective 70%, 30%, and 10% data selection rates.

5.4. Qualitative Results

We show the highest ranked ZCore images for EuroSAT80, CIFAR100, and ImageNet in Fig. 7. Across all dataset sizes and settings, the highest-ranked images are all unique, demonstrating that the embedding-based coverage score successfully promotes diverse examples from the full dataset without labels or training. In fact, ZCore achieves full class recall across all datasets and prune rates (full recall details and additional qualitative results in the Supplementary). For the same three datasets, we also show the lowest-ranked ZCore images with their nearest embedding neighbors in Fig. 8. For each dataset, the lowest-ranked images are highly redundant, which demonstrates that the embedding-based redundancy score is penalizing and subsequently pruning redundant examples from the full dataset.

5.5. Ablation Study

We provide ZCore ablative results in Tab. 3. When using a single model to generate our embedding space (\mathcal{Z}), ResNet18 outperforms CLIP, but neither perform as well as the standard concatenated setting. We also test a DINOv2 ViT-B-14 model [33], which shows that ZCore maintains near full performance even with a self-supervised zero-shot embedding space. Gaussian sampling (\mathbf{z}) outperforms Uniform but does not match Triangular performance. Given the close performance gap between Triangular and Gaussian sampling, we postulate that exploring additional sampling strategies is a promising area for future work. Decreasing or increasing the subspace sampling dimension (m) leads to lower performance, with high-dimension samples performing worst in terms of *both* accuracy and runtime (see Fig. 13 in Supplementary). We postulate the accuracy decrease occurs because the L_1 distance metric in Eq. (5) is less meaningful in higher-dimensional space [35]. Nonetheless, the L_1 metric outperforms the L_2 and \cos distance ablations.

For the importance score, we test multiple redundancy settings (α, β) and find that ZCore performance is robust to these parameter changes. Removing the redundancy score entirely (s^R) decreases performance more substantially than any other ablative configuration, validating our design choice to penalize nearest neighbors in each embedding subspace to reduce redundancy. Replacing embedding coverage sample selection with a uniformly random sample k also decreases performance, which validates our design choice to emphasize selection of examples that individually

occupy larger, lower-density embedding areas. Finally, removing random initialization (s) or the score loss weight w from model training decreases performance.

We plot the runtime and accuracy performance of ZCore over a wide range of score iterations in Fig. 9. We measure coreset selection runtime using a M3 Max-equipped laptop. The largest accuracy increase occurs when the coverage and redundancy score iterations (T) increase from 100 to 1,000, at which point, with the redundancy score reaching 1,000 neighbors per iteration, the score likely reaches most of the 50,000 CIFAR100 candidate training examples. The accuracy peaks at the default 1M iteration setting then converges on a slightly lower accuracy with increasing iterations. Notably, the default setting takes less than 400 s on a standard laptop, making ZCore a computationally efficient alternative to training-based coreset selection methods.

Additional ablative studies for ImageNet embedding models are provided in the Supplementary Material.

6. Conclusion

Recent state-of-the-art coreset selection methods improve performance in experiments by using labels and training on candidate data prior to selection. However, the majority of real-world data are unlabeled. To address this, we developed a coreset selection method, ZCore, that maintains state-of-the-art performance without labels or training. Instead, ZCore selects data using a novel iterative subspace sampling technique that operates on a high-dimensional embedding space representation of unlabeled data. In our experiments, we find that embeddings can be generated by a variety of previously-trained, off-the-shelf foundation models, including those originally trained with self-supervision. Not training on candidate data reduces computation, and unlabeled selection enables data- and label-efficient downstream model training on the selected coreset.

To evaluate our approach, we include ten state-of-the-art methods in experiments that select coresets, train downstream models, and evaluate subsequent validation accuracy on four datasets. Our experiment scale ranges from full datasets of over a million images all the way down to pruned coresets of 270 training images. In these experiments, our method outperforms all others save one, which uses full ground truth labels and model training on all data before coreset selection as well as prune rate-specific tuning on the validation set for configuration. In contrast, ZCore uses constant algorithmic settings across all experiments, making it generalizable, and selects coresets without labels or training, making it much more efficient for coreset selection at the rapidly expanding scale of our current deep learning era. From these results, ZCore establishes a new state-of-the-art approach to coreset selection.

We discuss future work in the Supplementary Material.

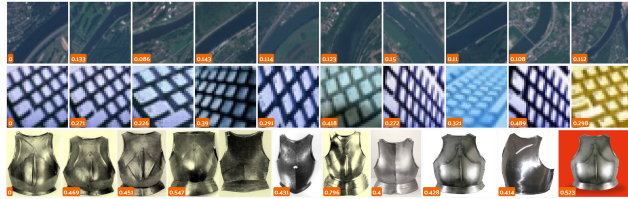


Figure 8. **Lowest ZCore Selection Score** (column 1) with nine nearest neighbors in the full embedding space for EuroSAT80 (top), CIFAR100 (middle), and ImageNet (bottom).

Table 3. Comparison of **ZCore ablations** on CIFAR 100 with ResNet18. Accuracy is the mean across 70%, 50%, 30%, 20%, and 10% data rates over five repeat trials. “ResNet18, CLIP” is the default concatenated embedding space using both foundation models off-the-shelf. Additional details in Supplementary Tab. 8.

Full Method / Ablation	Setting	Accuracy
ZCore	ResNet18, CLIP	65.77
Zero-Shot Embedding Space (Z)	ResNet18 [17]	65.52
	CLIP [39]	64.84
	DINOv2 [33]	65.61
ZCore	Triangular	65.77
Sampling Distribution (z)	Gaussian	65.75
	Uniform	64.84
ZCore	2	65.77
Subspace Sampling Dimensions (m)	1	64.59
	3	65.10
	10	63.27
	100	62.20
ZCore	L_1	65.77
Distance Metric (Eq. (5), Eq. (7))	L_2	65.60
	cos	64.48
ZCore	1,000	65.77
Number of Nearest Neighbors (α)	100	65.68
	10,000	65.72
ZCore	4	65.77
Distance Penalty Exponent (β)	3	65.64
	5	65.74
ZCore	Full Score	65.77
Random Coverage Sample (k)	Partial Score	64.74
No Redundancy Score (s^R)	Partial Score	61.71
No Random Initialization (s)	Partial Score	65.66
No Score Loss Weight (w)	Partial Score	63.53

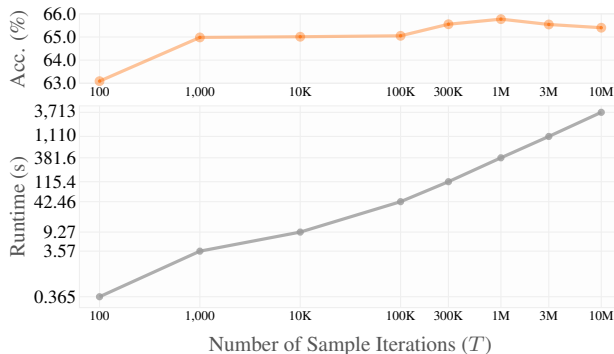


Figure 9. Comparison of number of sample iterations vs. accuracy (top) and **runtime** (bottom) on CIFAR100. Accuracy is the mean across 70%, 50%, 30%, 20%, and 10% data selection rates over five repeat trials. Runtime is selection time using a standard laptop.

References

- [1] Amro Abbas, Kushal Tirumala, Dániel Simig, Surya Ganguli, and Ari S Morcos. Semdedup: Data-efficient learning at web-scale through semantic deduplication. *arXiv preprint arXiv:2303.09540*, 2023. 2, 12
- [2] Dario Amodei, Danny Hernandez, GirishSastry, Jack Clark, Greg Brockman, and Ilya Sutskever. Ai and compute. 2018. 1
- [3] Jordan T. Ash, Chicheng Zhang, Akshay Krishnamurthy, John Langford, and Alekh Agarwal. Deep batch active learning by diverse, uncertain gradient lower bounds. In *International Conference on Learning Representations (ICLR)*, 2020. 2
- [4] Olivier Bachem, Mario Lucic, and Andreas Krause. Coresets for nonparametric estimation - the case of dp-means. In *Proceedings of the 32nd International Conference on Machine Learning (ICML)*, 2015. 2
- [5] J. Bernard, M. Hutter, M. Zeppelzauer, D. Fellner, and M. Sedlmair. Comparing visual-interactive labeling with active learning: An experimental study. *IEEE Transactions on Visualization and Computer Graphics*, 2018. 2
- [6] Trevor Campbell and Tamara Broderick. Bayesian coreset construction via greedy iterative geodesic ascent. In *Proceedings of the 35th International Conference on Machine Learning (PMLR)*, 2018. 12
- [7] George Cazenavette, Tongzhou Wang, Antonio Torralba, Alexei A. Efros, and Jun-Yan Zhu. Dataset distillation by matching training trajectories. In *Proceedings of the IEEE/CVF Conference on Computer Vision and Pattern Recognition (CVPR) Workshops*, 2022. 2
- [8] Chengliang Chai, Jiabin Liu, Nan Tang, Ju Fan, Dongjing Miao, Jiayi Wang, Yuyu Luo, and Guoliang Li. Goodcore: Data-effective and data-efficient machine learning through coreset selection over incomplete data. *Proc. ACM Manag. Data*, 2023. 12
- [9] Gui Citovsky, Giulia DeSalvo, Claudio Gentile, Lazaros Karydas, Anand Rajagopalan, Afshin Rostamizadeh, and Sanjiv Kumar. Batch active learning at scale. In *Advances in Neural Information Processing Systems (NeurIPS)*, 2021. 2
- [10] Cody Coleman, Christopher Yeh, Stephen Mussmann, Baharan Mirzasoleiman, Peter Bailis, Percy Liang, Jure Leskovec, and Matei Zaharia. Selection via proxy: Efficient data selection for deep learning. In *International Conference on Learning Representations (ICLR)*, 2020. 5, 6, 12, 14, 18
- [11] Marius Cordts, Mohamed Omran, Sebastian Ramos, Timo Rehfeld, Markus Enzweiler, Rodrigo Benenson, Uwe Franke, Stefan Roth, and Bernt Schiele. The cityscapes dataset for semantic urban scene understanding. In *Proceedings of the IEEE Conference on Computer Vision and Pattern Recognition (CVPR)*, 2016. 2
- [12] Jia Deng, Wei Dong, Richard Socher, Li-Jia Li, Kai Li, and Li Fei-Fei. Imagenet: A large-scale hierarchical image database. In *IEEE Conference on Computer Vision and Pattern Recognition (CVPR)*, 2009. 5
- [13] Alexey Dosovitskiy, Lucas Beyer, Alexander Kolesnikov, Dirk Weissenborn, Xiaohua Zhai, Thomas Unterthiner, Mostafa Dehghani, Matthias Minderer, Georg Heigold, Sylvain Gelly, Jakob Uszkoreit, and Neil Houlsby. An image is worth 16x16 words: Transformers for image recognition at scale. In *International Conference on Learning Representations (ICLR)*, 2021. 1
- [14] Thomas Elsken, Jan Hendrik Metzen, and Frank Hutter. Neural architecture search: A survey. *Journal of Machine Learning Research (JMLR)*, 2019. 1
- [15] Dan Feldman, Matthew Faulkner, and Andreas Krause. Scalable training of mixture models via coresets. In *Advances in Neural Information Processing Systems (NeurIPS)*, 2011. 2
- [16] Chengcheng Guo, Bo Zhao, and Yanbing Bai. Deepcore: A comprehensive library for coreset selection in deep learning. In *Database and Expert Systems Applications*, 2022. 2
- [17] Kaiming He, Xiangyu Zhang, Shaoqing Ren, and Jian Sun. Deep residual learning for image recognition. In *IEEE Conference on Computer Vision and Pattern Recognition (CVPR)*, 2016. 4, 8, 15
- [18] Muyang He, Shuo Yang, Tiejun Huang, and Bo Zhao. Large-scale dataset pruning with dynamic uncertainty. In *IEEE/CVF Conference on Computer Vision and Pattern Recognition (CVPR) Workshops*, 2024. 2, 3, 5, 6, 12, 18
- [19] Patrick Helber, Benjamin Bischke, Andreas Dengel, and Damian Borth. Eurosat: A novel dataset and deep learning benchmark for land use and land cover classification. *IEEE Journal of Selected Topics in Applied Earth Observations and Remote Sensing*, 2019. 5
- [20] Suyog Dutt Jain and Kristen Grauman. Predicting sufficient annotation strength for interactive foreground segmentation. In *IEEE International Conference on Computer Vision (ICCV)*, 2013. 2
- [21] Katrin Kirchhoff and Jeff Bilmes. Submodularity for data selection in machine translation. In *Proceedings of the 2014 Conference on Empirical Methods in Natural Language Processing (EMNLP)*, 2014. 12
- [22] Alex Krizhevsky. Learning multiple layers of features from tiny images. 2009. 5
- [23] Alex Krizhevsky, Ilya Sutskever, and Geoffrey E Hinton. Imagenet classification with deep convolutional neural networks. In *Advances in Neural Information Processing Systems (NeurIPS)*, 2012. 1
- [24] Liam Li and Ameet Talwalkar. Random search and reproducibility for neural architecture search. In *Proceedings of The 35th Uncertainty in Artificial Intelligence Conference*, 2020. 1
- [25] Jonathan Lorraine, Paul Vicol, and David Duvenaud. Optimizing millions of hyperparameters by implicit differentiation. In *Proceedings of the Twenty Third International Conference on Artificial Intelligence and Statistics*, 2020. 1
- [26] Mengyao Lyu, Jundong Zhou, Hui Chen, Yijie Huang, Dongdong Yu, Yaqian Li, Yandong Guo, Yuchen Guo, Liuyu Xiang, and Guiguang Ding. Box-level active detection. In *Proceedings of the IEEE/CVF Conference on Computer Vision and Pattern Recognition (CVPR)*, 2023. 16
- [27] Laurens van der Maaten and Geoffrey Hinton. Visualizing data using t-sne. *Journal of Machine Learning Research (JMLR)*, 2008. 15

- [28] Dougal Maclaurin, David Duvenaud, and Ryan Adams. Gradient-based hyperparameter optimization through reversible learning. In *Proceedings of the 32nd International Conference on Machine Learning (ICML)*, 2015. 1
- [29] Andrew McCallum and Kamal Nigam. Employing EM and pool-based active learning for text classification. In *International Conference on Machine Learning (ICML)*, 1998. 2
- [30] Leland McInnes, John Healy, Nathaniel Saul, and Lukas Grossberger. Umap: Uniform manifold approximation and projection. *The Journal of Open Source Software*, 2018. 4, 15
- [31] Nicholas Metropolis and Stanisław Ulam. The monte carlo method. *Journal of the American Statistical Association*, 44 (247):335–341, 1949. 4
- [32] B. E. Moore and J. J. Corso. Fiftyone. <https://github.com/voxel51/fiftyone>, 2020. 4, 15
- [33] Maxime Oquab, Timothée Darcet, Théo Moutakanni, Huy V. Vo, Marc Szafraniec, Vasil Khalidov, Pierre Fernandez, Daniel HAZIZA, Francisco Massa, Alaaeldin El-Nouby, Mido Assran, Nicolas Ballas, Wojciech Galuba, Russell Howes, Po-Yao Huang, Shang-Wen Li, Ishan Misra, Michael Rabbat, Vasu Sharma, Gabriel Synnaeve, Hu Xu, Herve Jegou, Julien Mairal, Patrick Labatut, Armand Joulin, and Piotr Bojanowski. DINOv2: Learning robust visual features without supervision. *Transactions on Machine Learning Research (TMLR)*, 2024. 7, 8, 15
- [34] Dongmin Park, Seola Choi, Doyoung Kim, Hwanjun Song, and Jae-Gil Lee. Robust data pruning under label noise via maximizing re-labeling accuracy. In *Advances in Neural Information Processing Systems (NeurIPS)*, 2023. 2
- [35] Jae Hyeon Park, Gyoomin Lee, Seunggi Park, and Sung In Cho. Not all classes stand on same embeddings: Calibrating a semantic distance with metric tensor. In *Proceedings of the IEEE/CVF Conference on Computer Vision and Pattern Recognition (CVPR)*, 2024. 7
- [36] Adam Paszke, Sam Gross, Francisco Massa, Adam Lerer, James Bradbury, Gregory Chanan, Trevor Killeen, Zeming Lin, Natalia Gimelshein, Luca Antiga, Alban Desmaison, Andreas Kopf, Edward Yang, Zachary DeVito, Martin Raison, Alykhan Tejani, Sasank Chilamkurthy, Benoit Steiner, Lu Fang, Junjie Bai, and Soumith Chintala. Pytorch: An imperative style, high-performance deep learning library. In *Advances in Neural Information Processing Systems (NeurIPS)*, 2019. 5
- [37] Mansheej Paul, Surya Ganguli, and Gintare Karolina Dziugaite. Deep learning on a data diet: Finding important examples early in training. In *Advances in Neural Information Processing Systems (NeurIPS)*, 2021. 5, 6, 12, 14, 18
- [38] Geoff Pleiss, Tianyi Zhang, Ethan Elenberg, and Kilian Q Weinberger. Identifying mislabeled data using the area under the margin ranking. In *Advances in Neural Information Processing Systems (NeurIPS)*, 2020. 5, 6, 12, 14, 18
- [39] Alec Radford, Jong Wook Kim, Chris Hallacy, Aditya Ramesh, Gabriel Goh, Sandhini Agarwal, Girish Sastry, Amanda Askell, Pamela Mishkin, Jack Clark, Gretchen Krueger, and Ilya Sutskever. Learning transferable visual models from natural language supervision. In *Proceedings of the 38th International Conference on Machine Learning (ICML)*, 2021. 4, 8, 15
- [40] Aditya Ramesh, Prafulla Dhariwal, Alex Nichol, Casey Chu, and Mark Chen. Hierarchical text-conditional image generation with clip latents. *arXiv preprint arXiv:2204.06125*, 2022. 1
- [41] Ozan Sener and Silvio Savarese. Active learning for convolutional neural networks: A core-set approach. In *International Conference on Learning Representations (ICLR)*, 2018. 2, 3
- [42] Burr Settles. Active learning. *Synthesis Lectures on Artificial Intelligence and Machine Learning*, 2012. 2
- [43] Eric Slyman, Stefan Lee, Scott Cohen, and Kushal Kafle. Fairdedup: Detecting and mitigating vision-language fairness disparities in semantic dataset deduplication. In *Proceedings of the IEEE/CVF Conference on Computer Vision and Pattern Recognition (CVPR)*, 2024. 2
- [44] Ben Sorscher, Robert Geirhos, Shashank Shekhar, Surya Ganguli, and Ari Morcos. Beyond neural scaling laws: beating power law scaling via data pruning. In *Advances in Neural Information Processing Systems (NeurIPS)*, 2022. 2, 3, 5, 6, 12, 14
- [45] Haoru Tan, Sitong Wu, Fei Du, Yukang Chen, Zhibin Wang, Fan Wang, and Xiaojuan Qi. In *Advances in Neural Information Processing Systems (NeurIPS)*, 2023. 2
- [46] Mariya Toneva, Alessandro Sordoni, Remi Tachet des Combes, Adam Trischler, Yoshua Bengio, and Geoffrey J. Gordon. An empirical study of example forgetting during deep neural network learning. In *International Conference on Learning Representations (ICLR)*, 2019. 2, 5, 6, 12, 14, 18
- [47] Kai Wang, Bo Zhao, Xiangyu Peng, Zheng Zhu, Shuo Yang, Shuo Wang, Guan Huang, Hakan Bilen, Xinchao Wang, and Yang You. Cafe: Learning to condense dataset by aligning features. In *Proceedings of the IEEE/CVF Conference on Computer Vision and Pattern Recognition (CVPR)*, 2022. 2
- [48] Kai Wei, Rishabh Iyer, and Jeff Bilmes. Submodularity in data subset selection and active learning. In *Proceedings of the 32nd International Conference on Machine Learning (ICML)*, 2015. 2
- [49] Max Welling. Herding dynamical weights to learn. In *Proceedings of the 26th Annual International Conference on Machine Learning (ICML)*, 2009. 2
- [50] Xiaobo Xia, Jiale Liu, Jun Yu, Xu Shen, Bo Han, and Tongliang Liu. Moderate coreset: A universal method of data selection for real-world data-efficient deep learning. In *International Conference on Learning Representations (ICLR)*, 2023. 2, 3, 5, 6, 12, 14, 18
- [51] Yichen Xie, Mingyu Ding, Masayoshi Tomizuka, and Wei Zhan. Towards free data selection with general-purpose models. In *Advances in Neural Information Processing Systems (NeurIPS)*, 2023. 2
- [52] Shuo Yang, Zeke Xie, Hanyu Peng, Min Xu, Mingming Sun, and Ping Li. Dataset pruning: Reducing training data by examining generalization influence. In *The Eleventh International Conference on Learning Representations (ICLR)*, 2023. 2

- [53] Ruonan Yu, Songhua Liu, and Xinchao Wang. Dataset distillation: A comprehensive review. *IEEE Transactions on Pattern Analysis and Machine Intelligence (TPAMI)*, 2024. [2](#)
- [54] Xin Zhang, Jiawei Du, Yunsong Li, Weiyang Xie, and Joey Tianyi Zhou. Spanning training progress: Temporal dual-depth scoring (tdds) for enhanced dataset pruning. In *IEEE/CVF Conference on Computer Vision and Pattern Recognition (CVPR)*, 2024. [2](#), [3](#), [5](#), [6](#), [12](#), [13](#), [14](#), [18](#)
- [55] Bo Zhao and Hakan Bilen. Dataset condensation with differentiable siamese augmentation. In *Proceedings of the 38th International Conference on Machine Learning (ICML)*, 2021. [2](#)
- [56] Bo Zhao and Hakan Bilen. Dataset condensation with distribution matching. In *Proceedings of the IEEE/CVF Winter Conference on Applications of Computer Vision (WACV)*, 2023. [1](#), [2](#)
- [57] Bo Zhao, Konda Reddy Mopuri, and Hakan Bilen. Dataset condensation with gradient matching. In *International Conference on Learning Representations (ICLR)*, 2021. [2](#)
- [58] Haizhong Zheng, Rui Liu, Fan Lai, and Atul Prakash. Coverage-centric coreset selection for high pruning rates. In *The Eleventh International Conference on Learning Representations (ICLR)*, 2023. [2](#), [3](#)
- [59] Haizhong Zheng, Elisa Tsai, Yifu Lu, Jiachen Sun, Brian R. Bartoldson, Bhavya Kailkhura, and Atul Prakash. ELFS: Label-free coreset selection with proxy training dynamics. In *The Thirteenth International Conference on Learning Representations (ICLR)*, 2025. [2](#), [3](#), [5](#), [6](#), [7](#), [12](#), [13](#), [18](#)

Zero-Shot Coreset Selection via Iterative Subspace Sampling

Supplementary Material

Reproducibility Statement

We provide detailed method and experiment descriptions in Secs. 4 and 5 of the main paper. We generate all ZCore experimental results from a single attempt of five consecutive trials with the exception of ImageNet, which is from a single attempt of one trial. Our paper’s code is publicly available at <https://github.com/voxel51/zcore>.

Experiment Datasets & External Baselines

To confirm that ZCore selects high-performing coresets, we perform experiments with ten state-of-the-art methods to select coresets, train downstream models, and evaluate performance on four datasets. Our experiments expand the recent work of Zhang et al. [54], which evaluated their coreset method with seven external baselines and three datasets.

Here, we provide detailed method descriptions for external baselines. **Entropy** selects examples with high entropy of predicted probabilities at the end of fully-supervised training on all candidate data [10]. **Forgetting** selects examples that change to being misclassified after correct classification the most times during training [46]. **EL2N** selects examples with high gradient magnitude using the L2 norm of error vectors [37]. **AUM** selects examples with high area under the margin, i.e., the probability gap between the target class and the next largest class across all epochs [38]. **Moderate** selects examples closest to the median class value in the full dataset trained model embedding space [50]. **Dyn-Unc** selects examples with high target class probability variance during training [18]. **TDDS** selects examples with high projected gradient variance across many epochs [54]. **Prototypes_{sup.}** selects examples based on difficulty, which is determined using k -means embedding clustering and the distance of each example to cluster centroids or *prototypes* [44]. Notably, **Prototypes_{sup.}** uses a supervised model trained on candidate data to generate embeddings while **Prototypes_{ss}** uses a self-supervised model [44]. **ELFS** uses an extensive framework of deep clustering on pretrained model embeddings to generate pseudo labels, subsequent full model training on pseudo labels, and finally selecting examples based on pseudo training dynamic-based scores without ground truth labels [59].

ZCore is the only method to make selections without ground truth labels *or* dataset training (see Fig. 2 of the

main paper) aside from **Random**, which selects examples with uniform random sampling. Furthermore we evaluate ZCore under constant algorithmic settings across a dataset and coreset selection scale greater than three orders of magnitude. Specifically, full dataset sizes span from 1.3 M to 2,700 examples and coreset sizes span from 896,817 to 270 examples (see Tab. 4.). To our knowledge, there is no precedent for this selection range of experiments and generalization in the coreset selection literature.

We also considered several other selection methods as baselines for our experiments. Unfortunately, as we will explain, these selection methods and many others are out of scope. Notably, our experiments use consistent prune rates for fair comparisons across coreset selection methods. On the other hand, **SemDeDup** [1], which selects coresets to remove semantic duplicates, uses configuration parameters that result in a prune rate that is unknown until *after* coreset selection experiments end. Perhaps due to this variable prune rate, the **SemDeDup** paper includes only a single data point as an external methodological comparison. **GIGA** constructs Bayesian coresets that scale log-likelihood optimality [6], but is originally applied to regression and would need to be modified for image classification. Other selection baselines originally applied to natural language processing would similarly require modification for our experiments [8, 21], which would materially change their functionality.

Expanded Coreset Selection Efficiency Details

We provide a detailed comparison of coreset selection efficiency in Tab. 5. In terms of runtime efficiency, ZCore selects data using embeddings generated from a single forward pass of off-the-shelf models, while TDDS and ELFS, which are representative of current SOTA methods, train on the entire dataset prior to coreset selection. However, training on data prior to selection takes substantially *more* time than any other process, whether using a laptop or GPU (see TDDS “Train Dynamics,” 52.3 hours and 1,540s respectively). Furthermore, ELFS requires repeat full data deep clustering *and* model training on pseudo labels to calculate scores for each prune rate. On the other hand, generating embeddings prior to selection is a one-time and parallizable operation that takes substantially less time than deep clustering, pretraining, or downstream model training, whether

Table 4. Comparison of **full training and coreset size** across all datasets. ZCore uses constant algorithmic settings across all experiments.

Dataset	Scale	Number of Classes	Full Dataset Training Size	Percent of Dataset Selected for Coreset				
				70%	50%	30%	20%	10%
ImageNet	Large	1,000	1,281,167	896,817	640,584	384,350	256,233	128,117
CIFAR100	Medium	100	50,000	35,000	25,000	15,000	10,000	5,000
CIFAR10	Medium	10	50,000	35,000	25,000	15,000	10,000	5,000
EuroSAT80	Medium	10	21,600	15,120	10,800	6,480	4,320	2,160
EuroSAT40	Small	10	10,800	7,560	5,400	3,240	2,160	1,080
EuroSAT20	Small	10	5,400	3,780	2,700	1,620	1,080	540
EuroSAT10	Small	10	2,700	1,890	1,350	810	540	270

Table 5. **Comparison of Coreset Selection Efficiency** on CIFAR100 for 70%, 30%, and 10% data rates. Selection “Total” is the runtime to generate all three coresets. Notably, ZCore uses the same score across all settings, while TDDS uses a unique validation-tuned setting for each prune rate (see Fig. 2). ELFS also uses a unique hyperparameter-tuned setting for each prune rate and additionally requires full-data deep clustering, pseudo training dynamics generation, and score calculation for each prune rate. Runtimes use a standard M3 Max-equipped “Laptop” or a single L40S “GPU” on a Lambda Scalar. ELFS hardware requirements prohibit laptop experiments. Following the protocol of TDDS [54], downstream model training at a 10% data rate on a GPU takes longer than 30% due to a reduced batch size.

Compute Hardware	Selection Runtime (s)				Total	Model Train Time (s)			Selection + Train Time (s)			Total Labels		
	Components			ZCore Score		70%	30%	10%	70%	30%	10%	70%	30%	10%
ZCore	Embedding Generation			ZCore Score										
	ResNet18	CLIP	Parallel											
Laptop	635	6,471	6,471	382	6,853	130,503	64,877	41,711	137,356	71,730	48,564	35K	15K	5K
GPU	145	97.0	145	54.7	199.8	990	589	643	1,190	789	843	35K	15K	5K
TDDS	Train Dynamics		TDDS Score											
		70%	30%	10%										
Laptop	188,295	27.0	25.5	0.9	188,296	130,503	64,877	41,711	318,825	253,198	230,008	50K	50K	50K
GPU	1,540	22.6	20.9	1.3	1,541	990	589	643	2,553	2,150	2,184	50K	50K	50K
ELFS	DINO Embed	Deep Cluster	Pseudo Train	ELFS Score										
GPU	111	1,093	1,476	30.3	7,908	990	589	643	3,701	3,300	3,353	35K	15K	5K
TDDS / ZCore Runtime & Label Requirement Ratio														
Laptop	—	—	—	—	27.5	—	—	—	2.32	3.53	4.74	1.43	3.33	10.0
GPU	—	—	—	—	7.7	—	—	—	2.14	2.72	2.59	1.43	3.33	10.0
ELFS / ZCore Runtime Requirement Ratio														
GPU	—	—	—	—	39.6	—	—	—	3.11	4.18	3.98	1.00	1.00	1.00

on the laptop or GPU (see ZCore “Embedding Generation,” 1.8 hours and 145s respectively).

From the results in Tab. 5, ZCore selects the three coresets $27.5\times$ faster than TDDS on a laptop and $39.6\times$ faster than ELFS on a GPU. Importantly, as discussed in Sec. 5.3, the relative time to implement ZCore is even faster. Reason being, ZCore uses the same settings across all datasets and the same score across all prune rates. On the other hand, both comparison methods perform parameter searches on *each* dataset and prune rate to determine their final dataset- and prune-specific settings. It is cost-prohibitive to replicate the hyperparameter search of each comparison method for our experiments in Tab. 5, but ELFS’s developers report that it takes approximately 17 hours using four A6000 GPUs to find a single prune rate setting on ImageNet [59].

In terms of label efficiency, TDDS, like many SOTA methods, uses ground truth labels on all candidate data prior to coreset selection. On the other hand, ZCore and ELFS se-

lect data without any ground truth labels. Accordingly, labels are only required during downstream model training for the selected coreset if the model is fully-supervised. Thus, TDDS requires 1.43, 3.33, and $10\times$ more labels than ZCore to train downstream models at the respective 70%, 30%, and 10% data selection rates in Tab. 5.

Class Recall after ZCore Selection

We provide the class recall of ZCore selections across all datasets and data selection rates of the main paper in Tab. 6. Notably, ZCore achieves 100% recall across all datasets and original data selection rates (10-70%). In addition to the main paper’s quantitative and qualitative results (Secs. 5.2 and 5.4), ZCore’s reliable class recall further establishes the viability of using iterative subspace sampling (Sec. 4) to achieve coreset data coverage without labels or training.

As an additional challenge, we also provide the class re-

Table 6. **ZCore Coreset Class Recall** after selection on all datasets. ZCore achieves 100% class recall in all the main paper’s experiments (**10-70%**, middle), so we include a few minimal selection rates as an added challenge (**0.5-5%**, right). Recall % is mean across all trials.

Dataset	Number of Classes	Full Dataset Training Size	Class Recall (%) at					Class Recall (%) at				
			Original Data Selection Rates (10-70%)					Minimal Data Rates (0.5-5%)				
			70%	50%	30%	20%	10%	5%	2%	1%	0.5%	
ImageNet	1,000	1,281,167	100%	100%	100%	100%	100%	100%	100%	100%	100%	100%
CIFAR100	100	50,000	100%	100%	100%	100%	100%	100%	100%	99%	92%	75%
CIFAR10	10	50,000	100%	100%	100%	100%	100%	100%	100%	100%	100%	100%
EuroSAT80	10	21,600	100%	100%	100%	100%	100%	100%	100%	100%	96%	88%
EuroSAT40	10	10,800	100%	100%	100%	100%	100%	100%	100%	90%	86%	78%
EuroSAT20	10	5,400	100%	100%	100%	100%	100%	100%	98%	90%	76%	66%
EuroSAT10	10	2,700	100%	100%	100%	100%	100%	100%	92%	82%	64%	58%

Table 7. Comparison of coreset selection methods using downstream model validation on **ImageNet**. Full dataset training on the ResNet32 model training achieves 73.54% accuracy. A corresponding results plot is provided in Fig. 5 of the main paper.

% of Data Selected	30%	20%	10%	Mean / Rel. Rand.
Unlabeled Coreset Selection without Training				
ZCore _{CLIP}	64.42	61.39	53.54	59.78 +0.59
Random	64.19	60.76	52.63	59.19 +0.00
Unlabeled Coreset Selection with Self-Supervised Training				
Prototypes _{SS} [44]	60.42	53.73	38.06	50.74 -8.45
Labeled Coreset Selection with Training-based Pruning				
TDDS [54]	64.69	62.56	53.91	60.39 +1.19
ZCore _{ResNet18, CLIP}	64.43	61.31	53.99	59.91 +0.72
Forgetting [46]	64.29	62.01	52.14	59.48 +0.29
Moderate [50]	64.04	61.35	52.45	59.28 +0.09
ZCore _{ResNet18}	63.37	60.57	52.97	58.97 -0.22
Entropy [10]	62.34	56.80	43.39	54.18 -5.02
Prototypes _{Sup.} [44]	53.59	42.25	22.41	39.42 -19.77
EL2N [37]	46.92	32.68	15.90	31.83 -27.36
AUM [38]	39.34	23.64	11.70	24.89 -34.30

call of ZCore selections on a few minimal data selection rates beyond those of the main paper (0.5-5%). Notably, ZCore maintains 100% class recall all the way down to a 0.5% data selection rate on CIFAR10 and even ImageNet, which has 1,000 classes. On the other hand, class recall drops below 100% for datasets with fewer initial images per class (e.g., CIFAR100 recall is 99% at a 2% data rate) or small datasets with much smaller corresponding coresets (EuroSAT10, EuroSAT20 at 5% data rates). Predictably, the lowest recall of 58% occurs on EuroSAT10 at a 0.5% data rate, which is selecting for a coreset of only 14 images.

ImageNet Embedding Ablations

ZCore selects coreset data using embeddings from “off-the-shelf” foundation models that were trained before this work and remain static. Notably, a component of the default embeddings (ResNet18) is previously trained on ImageNet. On

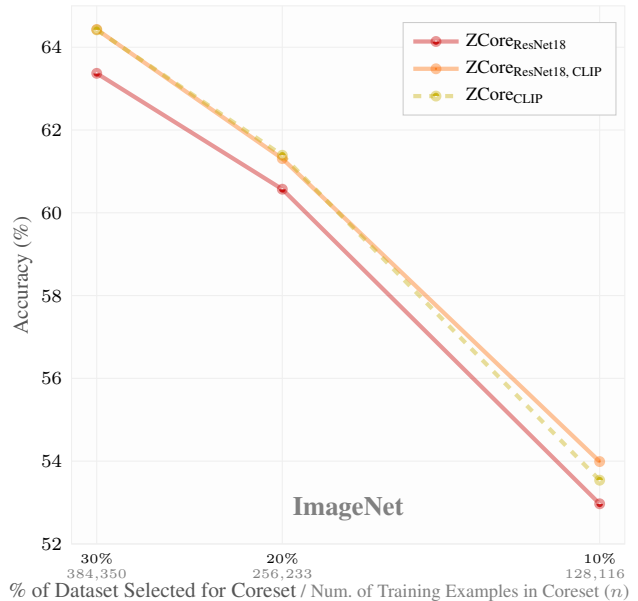


Figure 10. Comparison of coreset selection using downstream model validation on **ImageNet** for ZCore embedding ablations.

the other hand, we made a methodological commitment to use constant ZCore settings across all datasets and selection rates in our experiments, which includes consistent foundation models for embeddings.

To understand the relative contribution of ResNet18 embeddings for coreset selection on ImageNet, we perform an additional ablative experiment with ResNet18- and CLIP-only embeddings (see ZCore_{ResNet18} and ZCore_{CLIP} in Tab. 7 and Fig. 10). Notably, ZCore selections using CLIP-only embeddings are outperformed by *all* other embedding settings on CIFAR100 (see Tab. 3 in the main paper). On the other hand, ZCore_{CLIP} selections on ImageNet outperform ZCore_{ResNet18} across all data selection rates, despite ResNet18 pre-training on ImageNet. Furthermore, ZCore_{CLIP} performs comparably to the concatenated ZCore_{ResNet18, CLIP} setting on ImageNet, validating that ZCore is state-of-the-art for coreset selection without labels or training on candidate data across all experiment settings.

Table 8. Comparison of **ZCore** ablations on CIFAR 100 with ResNet18. Accuracy is the mean across 70%, 50%, 30%, 20%, and 10% data rates over five repeat trials. “ResNet18, CLIP” is the default concatenated embedding space using both models off-the-shelf.

Ablation	Zero-shot	Dimension	Sampling	Distance	Redundancy	Use Full	CIFAR100		
	Embedding Model	Reduction	Distribution	Dimensions	Metric	Neighbors		Exponent	Score
Full Method (ZCore)	ResNet18, CLIP	ZD	Triangular	2	L_1	1,000	4	Yes	65.77
Embedding Space (Z)	ResNet18 [17]	ZD	Triangular	2	L_1	1,000	4	Yes	65.52
	CLIP [39]	ZD	Triangular	2	L_1	1,000	4	Yes	64.84
	DINOv2 [33]	ZD	Triangular	2	L_1	1,000	4	Yes	65.61
Embedding Dimension Reduction (\hat{Z})	ResNet18, CLIP	PCA	Triangular	2	L_1	1,000	4	Yes	65.55
	ResNet18, CLIP	t-SNE [27]	Triangular	2	L_1	1,000	4	Yes	65.62
	ResNet18, CLIP	UMAP [30]	Triangular	2	L_1	1,000	4	Yes	62.43
Sampling Distribution (z)	ResNet18, CLIP	ZD	Gaussian	2	L_1	1,000	4	Yes	65.75
	ResNet18, CLIP	ZD	Uniform	2	L_1	1,000	4	Yes	64.84
Subspace Sampling Dimensions (m)	ResNet18, CLIP	ZD	Triangular	1	L_1	1,000	4	Yes	64.59
	ResNet18, CLIP	ZD	Triangular	3	L_1	1,000	4	Yes	65.10
	ResNet18, CLIP	ZD	Triangular	10	L_1	1,000	4	Yes	63.27
	ResNet18, CLIP	ZD	Triangular	100	L_1	1,000	4	Yes	62.20
Distance Metric (Eq. (5), Eq. (7))	ResNet18, CLIP	ZD	Triangular	2	L_2	1,000	4	Yes	65.60
	ResNet18, CLIP	ZD	Triangular	2	cos	1,000	4	Yes	64.48
Number of Nearest Neighbors (α)	ResNet18, CLIP	ZD	Triangular	2	L_1	100	4	Yes	65.68
	ResNet18, CLIP	ZD	Triangular	2	L_1	10,000	4	Yes	65.72
Distance Penalty Exponent (β)	ResNet18, CLIP	ZD	Triangular	2	L_1	1,000	3	Yes	65.64
	ResNet18, CLIP	ZD	Triangular	2	L_1	1,000	5	Yes	65.74
Random Coverage Sample (k)	NA	NA	NA	NA	L_1	1,000	4	No	64.74
No Redundancy Score (s^R)	ResNet18, CLIP	ZD	Triangular	2	L_1	NA	NA	No	61.71
No Random Initialization (s)	ResNet18, CLIP	ZD	Triangular	2	L_1	1,000	4	No	65.66
No Score Loss Weight (w)	ResNet18, CLIP	ZD	Triangular	2	L_1	1,000	4	No	63.53

Embedding Dimension Reduction Ablations

For dimension reduction, ZCore iteratively slices random subsets of the full embedding space to generate numerous subspace distributions, which are then sampled to find valuable examples based on coverage and redundancy (see Fig. 1 and Sec. 4 of the main paper for details). However, there are several alternative dimension reduction methods that are applicable to this work, including Principal Component Analysis (PCA), t-distributed Stochastic Neighbor Embedding (t-SNE) [27], and Uniform Manifold Approximation and Projection (UMAP) [30]. Notably, PCA maximizes variance to preserve pairwise global embedding distances while t-SNE and UMAP better preserve local embedding distances (see McInnes *et al.* for additional details and experiment comparisons [30]).

To validate the design decision to use ZCore’s iterative embedding dimension reduction technique, we provide experiment ablations using PCA, t-SNE, and UMAP as alternative embedding reduction processes for subsequent sampling and ZCore score generation in Tab. 8. Notably, the proposed ZCore dimension reduction technique ($\hat{Z} = ZD$ in Eq. (4)) outperforms all three dimension reduction alternatives. Nonetheless, the t-SNE and PCA ablations exhibit good performance, indicating that the subsequent ZCore processes for coverage and redundancy scoring are relatively robust to changes in the underlying dimension reduction technique used. From the results, we do not recom-

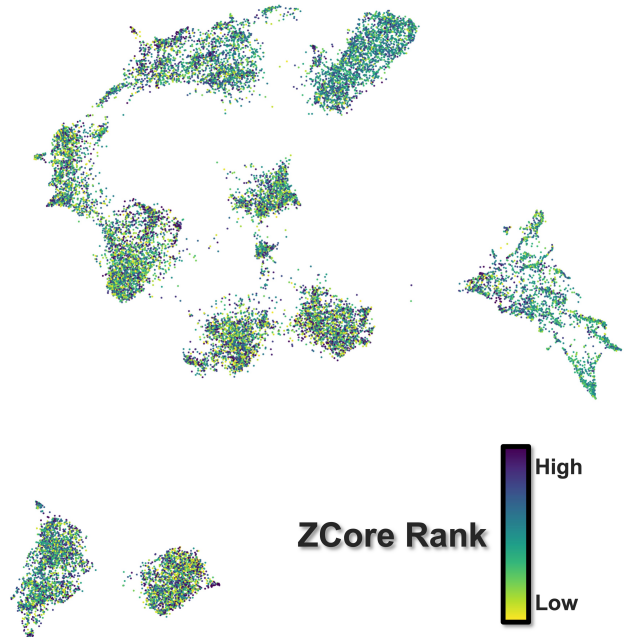


Figure 11. **ZCore Coreset Rank Visualization** for EuroSAT80. Model embeddings and 2D approximation of the full embedding space generated using the FiftyOne Library and UMAP [30, 32].

mend UMAP as an alternative dimension reduction technique for ZCore, but we still find UMAP to be an excellent tool for embedding space visualization (see Fig. 11).

Supplementary Figures & Tables

To supplement the evaluation in Sec. 5 of the main paper, we provide several additional figures and tables.

First, we show the entire ZCore rankings for EuroSAT80 within a 2D manifold approximation of the full embedding space in Fig. 11. Second, we plot self-supervised DINOv2 model embeddings and corresponding sample distributions in Fig. 12. Third, we plot the runtime and accuracy performance of ZCore over a range of subspace sampling dimensions in Fig. 13. Fourth, we show the highest 30 ranked ZCore images for EuroSAT80 in Fig. 14, CIFAR100 in Fig. 15, and ImageNet in Fig. 16. We also show the lowest 30 ranked ZCore images for ImageNet in Fig. 17. Finally, we tabulate coreset selection results for CIFAR10 and CIFAR100 in Tab. 9 (evaluating selection for two medium-sized datasets), ImageNet in Tab. 7 (evaluating selection at a large scale), and all EuroSAT splits in Tab. 10 (evaluating selection of satellite images at a decreasing scale).

Future Work

For downstream model training experiments in Sec. 5.2, ZCore outperforms all prior coreset selection methods except for the state-of-the-art TDDS method. However, TDDS performance relies on several requirements that, although useful in experiment settings, limit applicability and efficiency at scale. Specifically, TDDS assumes all candidate data are labeled prior to selection (which is cost prohibitive), performs fully-supervised model training on all candidate data prior to selection (which is runtime prohibitive), and uses a hyperparameter search on the validation set to determine the final configuration used on a per-dataset and per-prune rate basis (which limits generalization). On the other hand, ZCore uses no labels or training on candidate data prior to selection (which is label *and* runtime efficient) and uses constant algorithmic settings across all experiments (which is generalizable). Despite these procedural differences, ZCore maintains competitive performance and even outperforms TDDS at a 10% selection rate on EuroSAT40 and ImageNet. Nonetheless, there remain several promising methodological avenues to improve ZCore and further advance the viability of coreset selection without labels, training, or parameter tuning.

First, although ZCore performance degrades relative to TDDS on the small EuroSAT20 and EuroSAT10 datasets at low selection rates, we find that ZCore performance improves with alternative settings (e.g., reducing the number of nearest neighbors for redundancy in Eq. (7)). Thus, one area of future work is developing adaptive iterative subspace sampling so that ZCore automatically adjusts with dataset size and data selection rate to improve performance in challenge settings.

Second, in addition to the coverage and redundancy

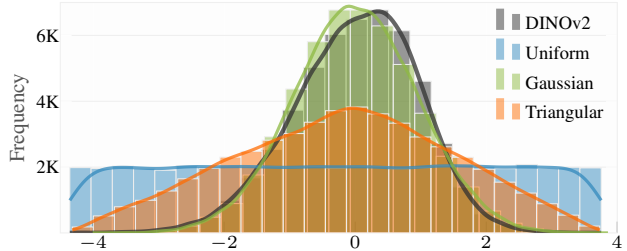


Figure 12. **Comparison of embeddings and sampling techniques.** DINOv2 is the first dimension embeddings for 50,000 CIFAR100 train set examples, while each corresponding distribution type is sampled 50,000 times. Corresponding plots for ResNet18 and CLIP are provided in Fig. 3 of the main paper.

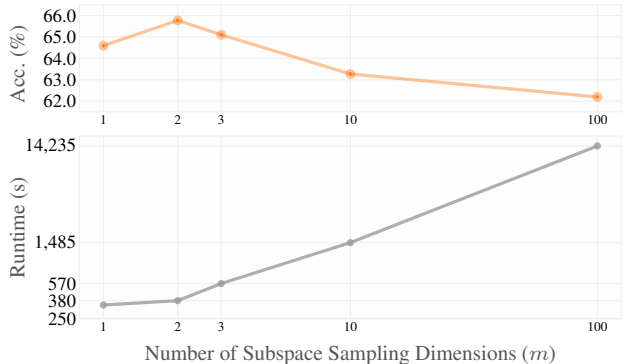


Figure 13. Comparison of number of **embedding subspace sample dimensions** (m) vs. accuracy (top) and **runtime** (bottom) on CIFAR100 with ResNet18. Accuracy is the mean across 70%, 50%, 30%, 20%, and 10% data selection rates over five repeat trials. Runtime is selection time using a M3 Max-equipped laptop.

scores developed in this paper, we postulate that there are many more label- and training-free features and metrics that can be developed to quantify coreset value for individual candidate examples. Expanding the set of metrics ZCore uses to consider each data example will likely make ZCore coreset selection more robust and performant across a wide range of datasets and data selection rates.

Finally, there is no domain-specific limitation to our method, so we can apply ZCore in other domains like point cloud and natural language and other problems like object detection and segmentation. However, each new domain and problem space will present new challenges *and* opportunities to improve ZCore. Taking object detection as one example, ZCore currently selects data using image-level embeddings but can also operate on object-level embeddings that are more representative of what downstream models will use for object detection. Furthermore, guiding data selection and annotation at an object level can lead to massive improvements in terms of overall human annotation time and downstream model performance [26]. Thus, we find that there are many exciting opportunities to expand and improve upon ZCore coreset selection in future work.



Figure 14. Top-30 ZCore Selection Scores (orange) for EuroSAT80.



Figure 15. Top-30 ZCore Selection Scores (orange) for CIFAR100.

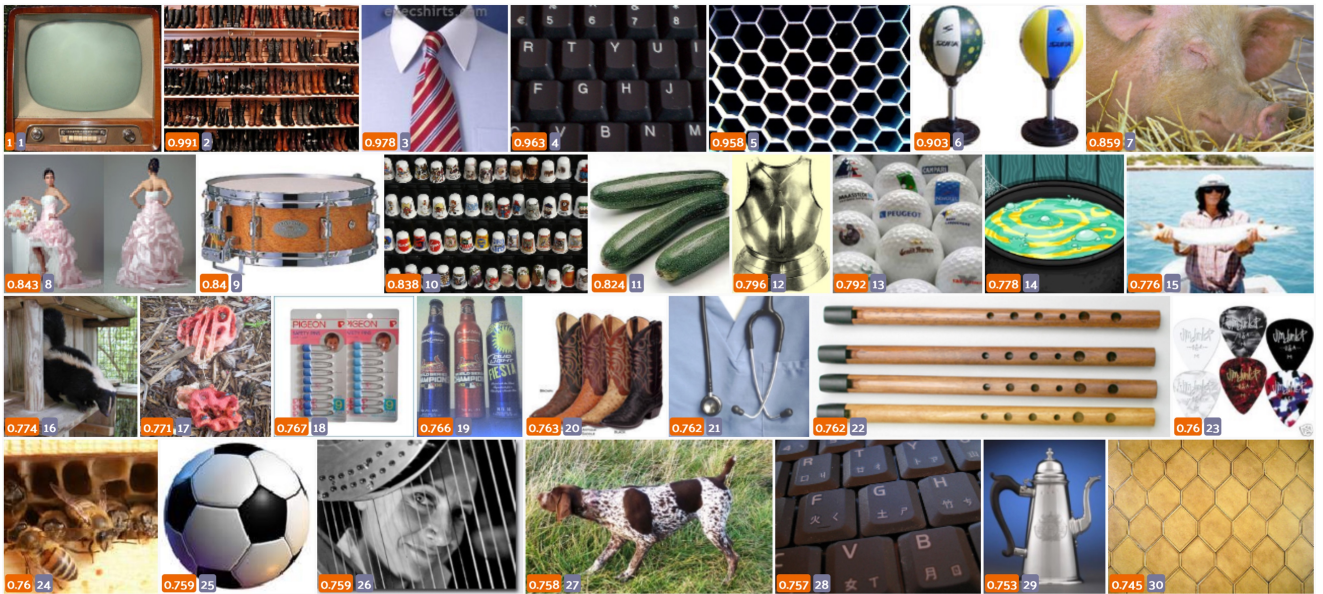


Figure 16. Top-30 ZCore Selection Scores (orange) for ImageNet.



Figure 17. Lowest-33 ZCore Selection Scores (orange) for ImageNet.

Table 9. Comparison of coresets selection methods using downstream model validation on **CIFAR10** and **CIFAR100**. Full dataset training on the ResNet18 model achieves 95.23% (CIFAR10) and 78.21% (CIFAR100) accuracy. “Rel. Rand.” is Mean accuracy across all data selection rates on both datasets relative to Random. A corresponding results plot is provided in Fig. 5 of the main paper.

% Data Selected	CIFAR10					CIFAR100					Mean Rel. Rand.
	70%	50%	30%	20%	10%	70%	50%	30%	20%	10%	
Unlabeled Coreset Selection without Training											
ZCore	94.58	93.46	90.97	89.06	84.18	76.04	72.87	65.92	61.92	52.11	78.11
	± 0.09	± 0.16	± 0.17	± 0.33	± 0.21	± 0.15	± 0.18	± 0.15	± 0.39	± 0.66	± 1.34
Random	94.58	93.38	90.61	88.87	83.77	75.53	71.95	64.59	57.79	46.68	76.78
	± 0.04	± 0.17	± 0.44	± 0.47	± 0.26	± 0.04	± 0.16	± 0.32	± 0.24	± 1.07	± 0.00
Unlabeled Coreset Selection with Self-Supervised Training											
ELFS [59]	94.04	92.61	90.37	88.04	82.39	74.10	70.36	63.83	58.51	47.42	76.17
ICLR 2025	± 0.14	± 0.26	± 0.07	± 0.38	± 0.35	± 0.15	± 0.18	± 0.56	± 0.20	± 1.32	-0.61
Labeled Coreset Selection with Training-based Pruning											
TDDS [54]	95.47	95.21	93.03	91.30	85.46	77.56	74.04	67.78	63.01	54.51	79.74
CVPR 2024	± 0.06	± 0.04	± 0.25	± 0.25	± 0.21	± 0.06	± 0.34	± 0.44	± 0.12	± 0.22	± 2.96
Moderate [50]	93.96	92.34	89.71	87.75	83.61	74.60	70.29	62.81	56.52	41.82	75.34
ICLR 2023	± 0.06	± 0.09	± 0.14	± 0.27	± 0.24	± 0.10	± 0.31	± 0.08	± 0.37	± 1.12	-1.43
Entropy [10]	94.45	91.90	86.24	83.49	72.06	72.39	64.44	50.73	42.86	29.56	68.81
ICLR 2020	± 0.07	± 0.16	± 0.26	± 0.21	± 0.81	± 0.20	± 0.36	± 0.86	± 0.25	± 0.54	-7.96
Forgetting [46]	95.45	95.05	89.14	76.18	45.87	77.38	70.76	49.92	38.42	25.82	66.40
ICLR 2019	± 0.24	± 0.05	± 2.04	± 3.18	± 1.87	± 0.09	± 0.40	± 0.28	± 1.13	± 0.52	-10.38
Dyn-Unc [18]	95.08	94.03	89.40	79.76	37.12	73.36	65.90	50.16	39.19	15.20	63.92
CVPR WS '24	± 0.02	± 0.14	± 0.13	± 1.09	± 1.12	± 0.10	± 0.25	± 0.47	± 0.27	± 0.41	-12.86
AUM [38]	95.44	95.19	91.19	69.60	34.74	77.35	68.17	31.69	18.43	9.29	59.11
NeurIPS 2020	± 0.09	± 0.09	± 0.63	± 3.11	± 0.11	± 0.18	± 0.52	± 0.34	± 0.47	± 0.27	-17.67
EL2N [37]	95.43	95.06	86.69	68.64	31.89	76.89	67.57	36.45	17.31	9.10	58.50
NeurIPS 2021	± 0.10	± 0.04	± 1.71	± 3.70	± 1.51	± 0.31	± 0.15	± 1.36	± 0.33	± 0.69	-18.27

Table 10. Comparison of coreset selection methods using downstream model validation on decreasing sized splits of **EuroSAT**. Full dataset training on the ResNet18 model achieves 98.59% (EuroSAT80), 98.20% (EuroSAT40), 97.36% (EuroSAT20), and 93.64% (EuroSAT10) accuracy. “Rel. Rand.” is Mean accuracy across all data selection rates relative to Random. “EuroSAT All” is Mean accuracy for all EuroSAT splits. EuroSAT10 10% selection has only 270 examples. A corresponding results plot is provided in Fig. 6 of the main paper.

Selection Method	Coreset Selection Requirements	Percent of Dataset Selected / Number of Examples					Mean Rel. Rand.
		70%	50%	30%	20%	10%	
EuroSAT All							
ZCore	Unlabeled Data	96.53	95.74	93.21	91.74	83.27	92.10 +1.14
Random	Unlabeled Data	94.56	92.91	89.80	87.88	83.61	90.96 +0.00
TDDS CVPR 2024	Full Training on Labeled Data	96.93	96.35	94.55	93.56	87.80	93.96 + 3.01
EuroSAT80 (21,600)							
ZCore	Unlabeled Data	15,120 98.32 ±0.08	10,800 98.15 ±0.13	6,480 97.72 ±0.13	4,320 97.31 ±0.17	2,160 95.80 ±0.18	97.46 +0.56
Random	Unlabeled Data	98.20 ±0.11	97.94 ±0.10	96.98 ±0.17	96.65 ±0.29	94.72 ±0.49	96.90 +0.00
TDDS CVPR 2024	Full Training on Labeled Data	98.62 ±0.05	98.58 ±0.11	98.43 ±0.03	98.09 ±0.10	96.28 ±0.11	98.00 +1.10
EuroSAT40 (10,800)							
ZCore	Unlabeled Data	7,560 97.59 ±0.05	5,400 97.53 ±0.16	3,240 96.45 ±0.12	2,160 96.06 ±0.19	1,080 92.94 ±0.55	96.11 +1.54
Random	Unlabeled Data	97.04 ±0.07	96.43 ±0.37	95.00 ±0.67	93.73 ±0.58	90.69 ±0.53	94.58 +0.00
TDDS CVPR 2024	Full Training on Labeled Data	97.97 ±0.09	98.06 ±0.06	97.55 ±0.08	96.79 ±0.16	92.78 ±0.27	96.63 +2.05
EuroSAT20 (5,400)							
ZCore	Unlabeled Data	3,780 96.49 ±0.16	2,700 95.45 ±0.22	1,620 92.60 ±0.29	1,080 91.80 ±0.70	540 80.39 ±3.91	91.35 +1.53
Random	Unlabeled Data	95.14 ±0.32	93.25 ±0.59	89.36 ±0.54	88.01 ±0.22	83.30 ±0.73	89.81 +0.00
TDDS CVPR 2024	Full Training on Labeled Data	96.94 ±0.10	96.45 ±0.07	93.86 ±0.56	94.70 ±0.35	86.94 ±0.55	93.78 +3.97
EuroSAT10 (2,700)							
ZCore	Unlabeled Data	1,890 93.71 ±0.23	1,350 91.82 ±0.23	810 86.08 ±1.16	540 81.77 ±2.68	270 63.96 ±2.76	83.47 +0.92
Random	Unlabeled Data	90.35 ±0.64	87.55 ±0.67	83.06 ±1.61	78.97 ±1.88	72.81 ±2.25	82.55 +0.00
TDDS CVPR 2024	Full Training on Labeled Data	94.62 ±0.09	92.92 ±0.33	89.41 ±0.52	85.56 ±0.67	74.74 ±2.02	87.45 +4.90